

## Impact of Dwell Angle on the Electromagnetic Torque Ripples of the Switched Reluctance Motor

G. Bhuvaneswari<sup>1</sup>, P. Srinivasa Rao, Sarit Guha Thakurta, and S.S. Murthy<sup>1</sup>

<sup>1</sup>*Indian Institute of Technology Delhi, New Delhi-110 016*

### ABSTRACT

Switched reluctance motors (SRM) are emerging as promising competitors to the vector-controlled induction motor (VCIM) drives and permanent magnet (PM) motor drives in the variable-speed drive market owing to their robust nature coupled with low cost, simplicity, and capability to operate in harsh environments. They are also suitable for nuclear and aerospace applications due to their low inertia and capability to be fed from a dc supply through a simple power converter. The principle of torque production in SRM makes rotor position information mandatory for effective control of the drive. The torque produced by any particular phase of the SRM is dependent upon the exciting current and the period during which the current is carried by that phase winding. The conduction period of any particular phase is termed as dwell angle when it is specified in terms of rotor angular position. In the present work, the SRM operation has been analysed in sensor mode and in sensor-less mode, paying special attention to the relationship between dwell angle and output torque ripple. The performance has been studied for different values of dwell angle and the resultant torque profile has been analysed. From the analysis, a methodology has been devised to deduce an appropriate value of dwell angle for minimising the torque pulsations, given the values of speed and load torque, thus improving the performance of the SRM drive.

**Keywords:** Commutation, dwell angle, sensor-less control, switched reluctance motor, SRM, electromagnetic torque

### 1. INTRODUCTION

Adjustable speed ac drives like vector-controlled (VC) and direct-torque controlled (DTC) induction motor drives, permanent magnet brushless (PMBL) motor drives and switched reluctance motor (SRM) drives are rapidly replacing conventional dc motors in variable-speed applications due to their ruggedness, higher torque to inertia ratio, and low maintenance requirements. Recent advances in the area of power semiconductor devices and circuit topologies has made this possible. Out of these adjustable-speed drives, SRM has gained tremendous importance

because of its simple control and capability to achieve extremely high speeds. The SRM has been employed in high-speed centrifuges, electric vehicles, and nuclear and aerospace applications. The major problem of the SRM is the large amount of ripples in its output torque that makes it very noisy. The torque and speed of the SRM can be controlled accurately only by exciting the phase windings at appropriate instants in accordance with the rotor position. This is done by a power electronic converter<sup>1</sup>. To obtain rotor position information, a resolver or an encoder is used. The addition of this device increases the cost and decreases the reliability of

the SRM, especially in hazardous environments and space applications<sup>2-3</sup>. To overcome these problems associated with the position sensors, several sensor-less techniques have been developed<sup>4-5</sup>. Irrespective of whether the SRM is operating with or without sensors, the period of conduction of the phase winding influences the torque production significantly. The period for which each of the phase windings carries current, when expressed in terms of rotor angular position, is known as the dwell angle. This paper analyses the performance of the SRM for different values of dwell angles and deduces a suitable value of dwell angle for a 8/6 SRM for both sensor and sensor-less operations, given the speed and load torque values. This optimum dwell angle should give minimum or zero value of negative torque in each phase so that the overall torque has minimum pulsations.

## 2. CONTROL OF SWITCHED RELUCTANCE MOTOR

The concept behind the operation of SRM is that any ferromagnetic material aligns itself along the minimum reluctance position. The SRM has doubly salient structure with different number of poles in the stator and rotor. Figure 1 shows the

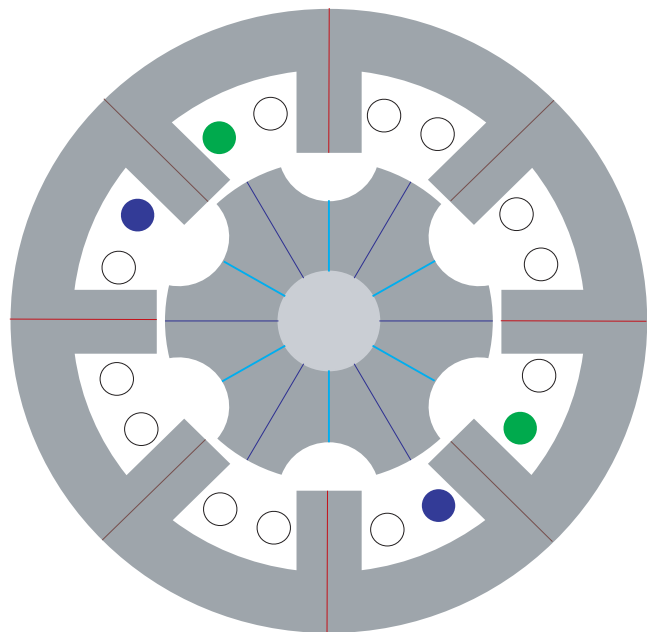


Figure 1. Cross-sectional view of 8/6 switched reluctance motor.

cross-sectional view of an 8/6 SRM. The stator has windings with diametrically opposite poles getting excitation at the same time. So, the 8 poles of the stator have 4-phase windings with the diametrically opposite poles having their windings connected in series. Normally, a mid-point converter is used for exciting the phase windings<sup>2</sup> as shown in Fig. 2. When the excitation changes over from phase 1 to phase 2 (from VV1 to VV2 in Fig. 2), the feedback diode ensures that a negative voltage is applied to the outgoing phase and hence, the flux across the outgoing phase diminishes faster. The electromagnetic torque produced<sup>6</sup> by the SRM is given by the equation

$$T_e = 0.5 * i^2 * (dL / d\theta) \tag{1}$$

where  $i$  is the current through the phase winding,  $(dL/d\theta)$  is the rate of change of inductance wrt

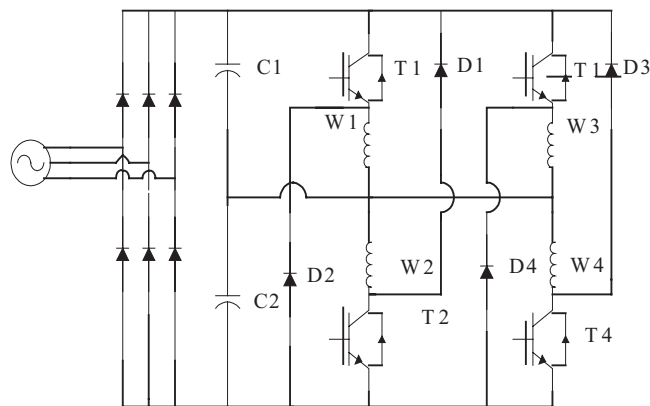


Figure 2. Mid-point converter for the control of switched reluctance motor.

the rotor position. This clearly indicates that if the current through any phase is a non-zero value while  $(dL/d\theta)$  is negative, braking torque would be produced. To minimise the torque pulsations, positive torque production has to be enhanced and negative torque production has to be strictly avoided. The period for which each phase winding conducts, i.e., the non-zero current period is known as the dwell time and the corresponding time expressed in terms of rotor angular position is known as dwell angle. The control of this dwell angle, thus, plays a significant role in deciding the resultant torque profile of the SRM drive.

### 3. ANALYSIS OF SRM OPERATION

To analyse the performance of SRM, the model of the entire drive system has been developed in both sensor and sensor-less modes in the simulation software<sup>7</sup> SIMULINK/MATLAB. The electrical and mechanical equations governing the operation of the SRM are

$$V = i * R + (d\psi / dt) \quad (2)$$

where  $V$  is the applied voltage,  $i$  is the phase current,  $R$  is the resistance of the phase winding and  $d\psi/dt$  is the rate of change of flux-linkage wrt time. If linear magnetisation characteristics are assumed for the SRM, then

$$\psi = L * i \quad (3)$$

where  $L$  is the phase inductance. The mechanical torque balance equation is

$$J * (d\omega / dt) = T_e - T_L \quad (4)$$

where  $J$  is the moment of inertia of the drive system,  $\omega$  is the angular velocity of the rotor,  $T_e$  is the electromagnetic torque given by Eqn (1) and  $T_L$  is the load torque. The above equations are translated into a block diagram as shown in Fig. 3. The model for one of the phases of SRM in sensor-mode is presented in Fig. 4. For different values

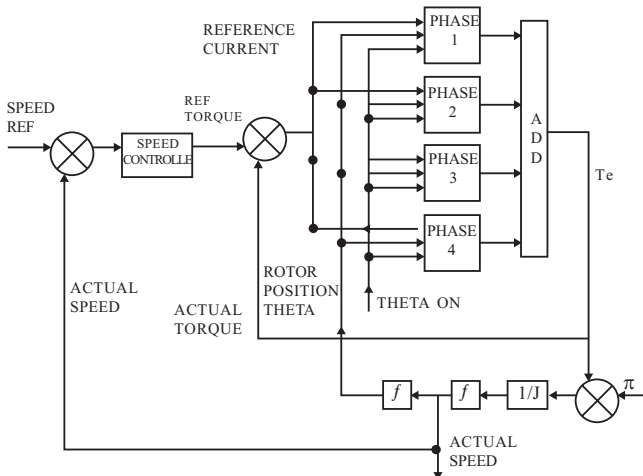


Figure 3. Block diagram of switched reluctance motor with position sensor.

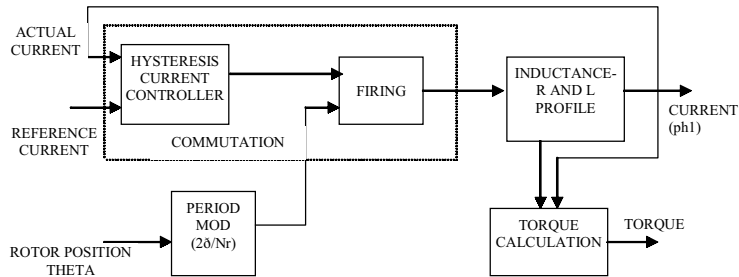


Figure 4. Model for phase 1 in simulation with sensor.

of  $\theta_{ON}$  (the angle at which conduction of a particular phase starts) and  $\theta_{OFF}$  (the angle at which the main switch is turned-off), the performance of the motor is analysed and the implications presented.

A novel method of sensor-less control also has been modelled as depicted in Fig. 5, which shows the model for one of the phases in sensor-less mode. The FE analysis of the SRM was carried out in the FE software called Maxwell-SV (Student version). The input to the package are the dimensions of the machine (as shown in Table 1), the excitation and the angular position of the rotor. The output is obtained in the form of flux plot as shown in Fig. 6. The actual values of the flux linkage at the rotor pole arc and the torque produced by the excited phase are also obtained from the FE analysis. The analysis was carried out for various values of phase currents and for different rotor positions. These plots are shown in Fig. 7.

Once the variations of torque and flux linkage wrt various excitation currents and  $\theta$  positions are obtained,  $T-i-\theta$  and  $\psi-i-\theta$  look-up-tables are formulated. For any applied voltage, the incremental flux linkage is given by the integral of voltage over the sampling

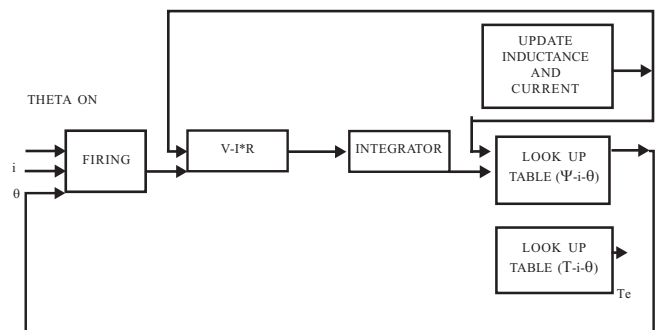
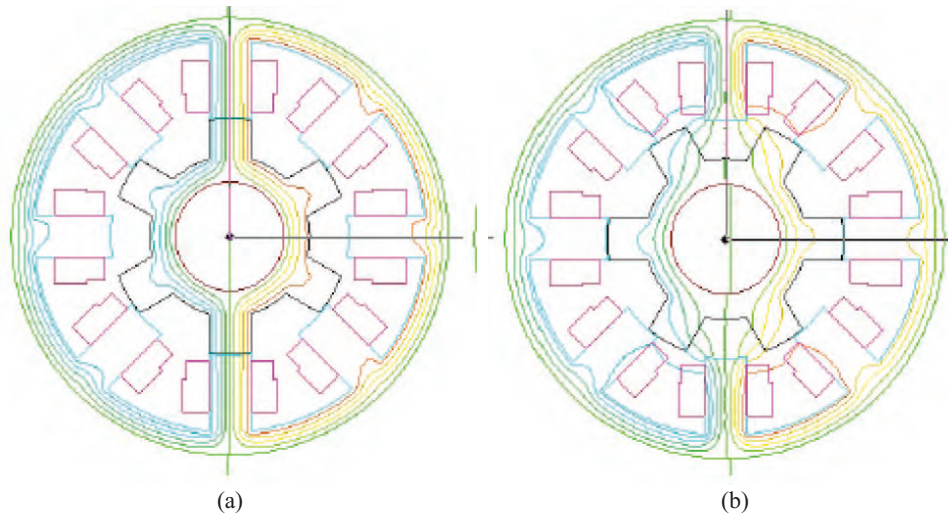


Figure 5. Model for phase 1 in sensor-less mode.

**Table 1. Dimensions of the 8/6 SRM used in the FE analysis using Maxwell-SV software**

| Stator                        |   | Rotor                   |                     |
|-------------------------------|---|-------------------------|---------------------|
| Winding                       | 4 phase, 8/6 pole                       | Rotor material          | Silicon sheet steel |
| Core material                 | Silicon sheet steel                     | Rotor pole tip dia (mm) | 95.5162             |
| Stator bore dia (mm)          | 96.2162                                 | Rotor pole arc (degree) | 21                  |
| Stator core outer dia         | 180                                     | Shaft dia (mm)          | 44.7                |
| Stator back iron width (mm)   | 10                                      | Air gap width (mm)      | 0.35                |
| Stator pole arc (degree)      | 21                                      | Stack depth (mm)        | 150                 |
|                               |   | Rotor pole height (mm)  | 16                  |
| <i>Stator coil dimensions</i> |   |                         |                     |
| Conductor size                | 1.8618 mm (dia for circular conductors) |                         |                     |



**Figure 6. Flux plot of the SRM at 5 A from FE analysis: (a) aligned position, and (b) unaligned position.**

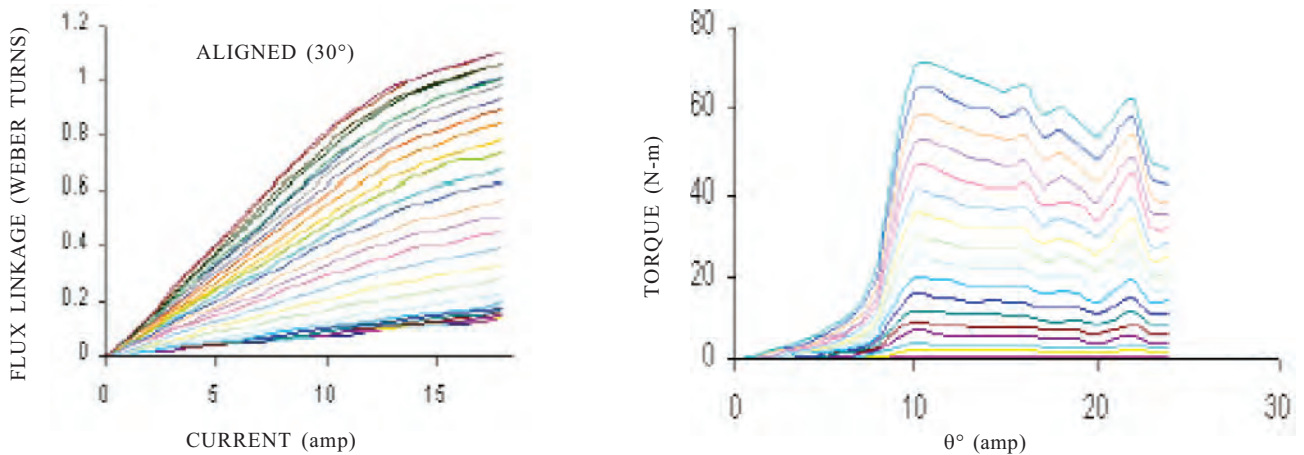


**Figure 7.  $\psi - i - \theta$  and  $T - i - \theta$  plots.**

time, if the resistance drop could be neglected. Hence, by measuring the voltage and current, the incremental flux linkage can be calculated as

$$\Delta\psi = \int (V - i * R) dt \quad (5)$$

Thus, from the applied voltage and current values, the flux-linkage is calculated, which is used to infer  $\hat{e}$  from the  $\theta - i - \hat{e}$  look-up table. Once  $\hat{e}$  is known, torque is obtained from the  $T - i - \hat{e}$  look-up table. Thus, the machine has been modelled in sensor-less mode. The parameters of the motor are presented in Table 2.

**Table 2. Specification of the switched reluctance motor OUTLON make (TASC drive)**

| Specification                    | Value                  |
|----------------------------------|------------------------|
| Power                            | 4 kW                   |
| Number of stator poles           | 8                      |
| Number of rotor poles            | 6                      |
| Speed                            | 1500 rpm               |
| Stator resistance per phase (52) | 0.747 $\Omega$         |
| Aligned (minimum) inductance     | 120 mH                 |
| Unaligned (maximum) inductance   | 10 mH                  |
| Moment of inertia ( $J$ )        | 0.008 kgm <sup>2</sup> |
| DC link voltage                  | 600 Vdc                |
| RMS current                      | 9 amp                  |
| Peak current                     | 18 amp                 |

#### 4. RESULTS

The analysis of the SRM was performed in the SIMULINK/ MATLAB environment for both sensor and sensor-less cases using the models described above. The simulations were carried out for different values of initial conduction angle ( $\hat{e}_{ON}$ ) and the commutation angle ( $\hat{e}_{OFF}$ ). As the SRM is a 8/6 one, the inductance profile repeats itself every 60° in one revolution (Fig. 8). The firing of a particular phase should be started a little ahead of the rising inductance region, so that the current in that phase should have reached a substantial value for producing the electromagnetic torque during the period where ( $dL/d\theta$ ) is positive. Similarly, to avoid negative torque production, current should be extinguished

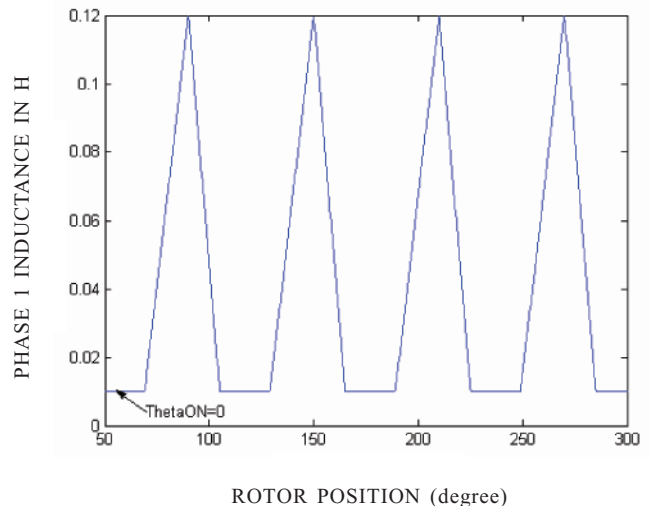


**Figure 8. Inductance variation of phase 1 with rotor position.**

before reaching the region where ( $dL/d\theta$ ) is negative.  $\theta_{ON}$  is considered to be zero if phase 1 is energised at the rotor position ( $\theta$ ) angle of 60° (as shown in Fig. 8).

The analysis of the drive was carried out for various values of  $\theta_{ON}$  and  $\theta_{OFF}$ . The speed, total torque, and torque in phase 1 obtained from the simulations are shown in the Figs 9 (a)–(c) for the drive operating with sensors. It can be seen that whenever the  $\theta_{ON}$  is very much delayed, sufficient amount of torque is not produced by the machine, as the current does not rise to a significant value in the positive ( $dL/d\theta$ ) region. Similarly, if  $\theta_{OFF}$  is delayed, the current persists in the negative ( $dL/d\theta$ ) region, thus contributing towards negative torque production. This causes large amount of oscillations in the torque. The Figs 10 (a)–(c) shows similar plots for the sensor-less case. The plots obtained in both sensor and sensor-less cases show similar trends in terms of the torque variations although the sensor-less case takes into account the saturation effect of the machine at higher currents and aligned position of the rotor. In reality, the phase inductance variation is not linear and should have reached a higher value much earlier than what is shown in Fig. 8. This would limit the rate of rise of phase winding current and thus an effect on the electromagnetic torque. The sluggish starting response in the sensor-less case may be attributed to this. The oscillations in the electromagnetic torque in sensor case is

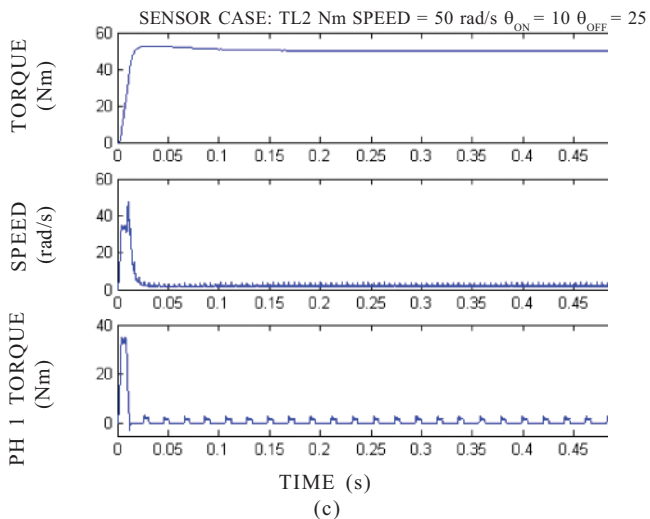
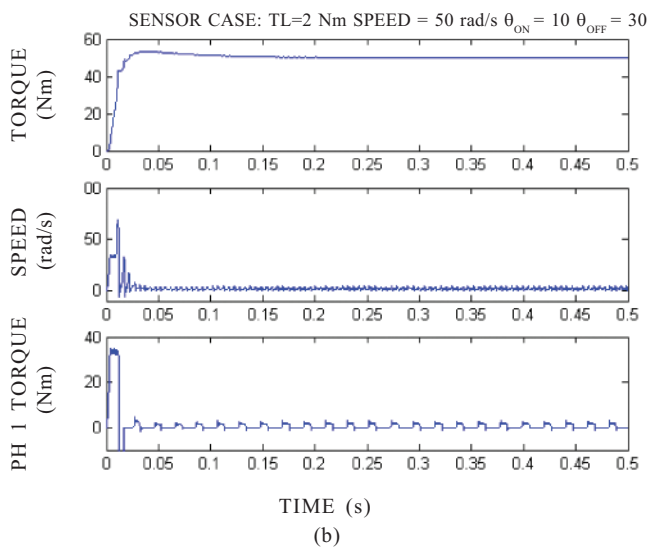
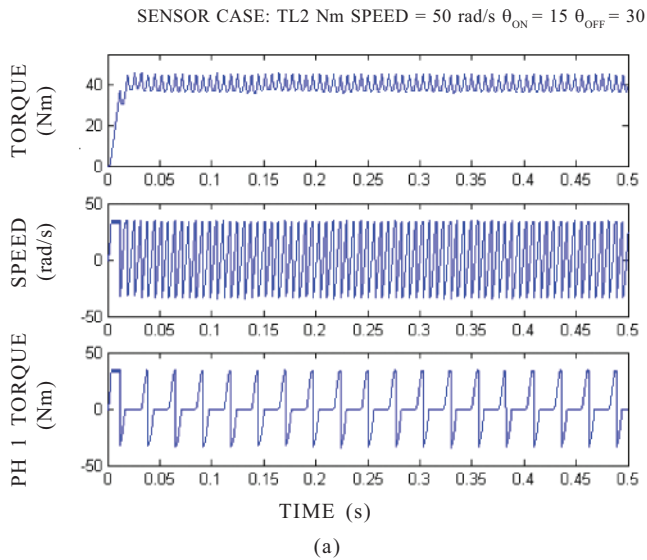


Figure 9. Responses of the SRM drive in sensor mode for various dwell angles (a-c).

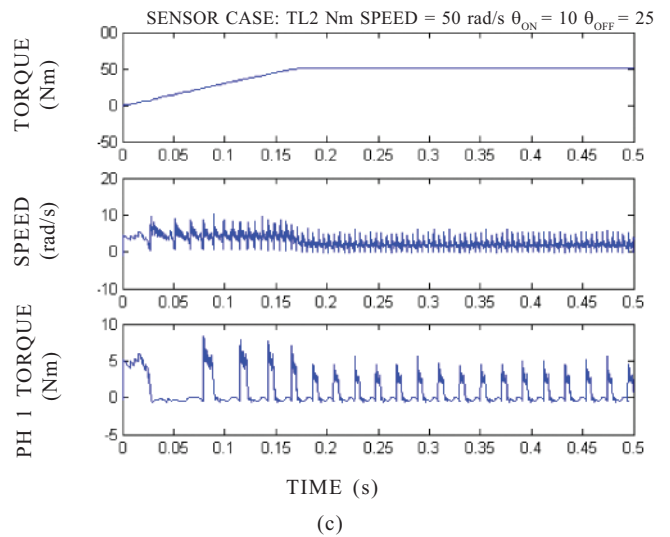
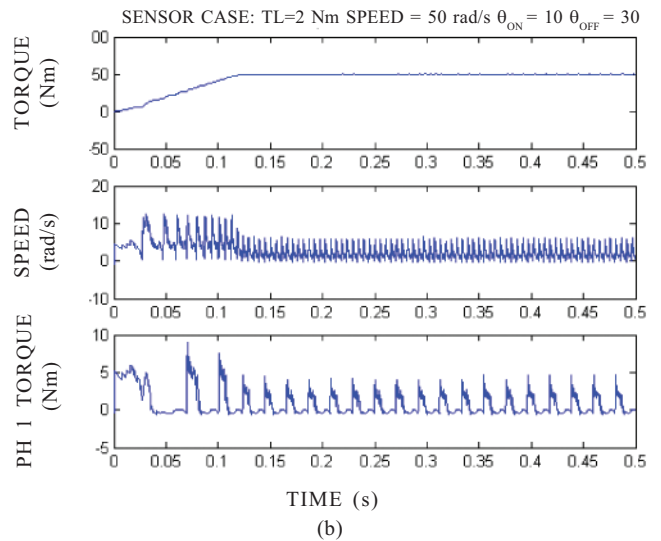
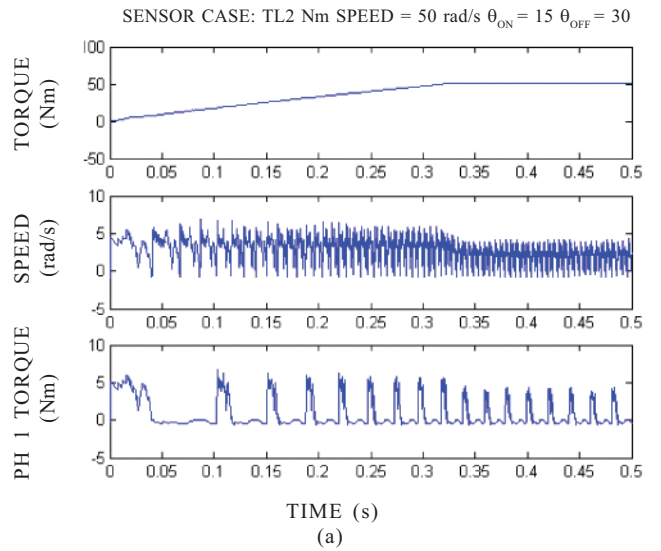
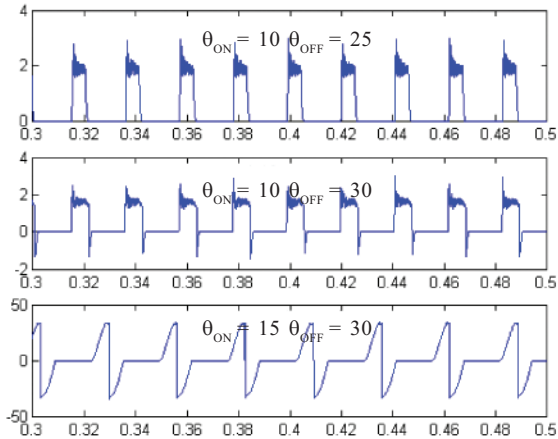


Figure 10. Response of the SRM drive in sensor-less mode for different dwell angles (a-c).

PHASE 1 TORQUE IN Nm IN SENSOR CASE FOR DIFFERENT DWELL ANGLES



**Figure 11.** Phase 1 torque of the SRM drive in sensor mode for different dwell angles with speed=50 rad/s and torque = 2 Nm.

higher as compared to the sensor-less case. This is due to the current variations being higher in sensor case, with the inductance reaching the maximum value at a slower rate as compared to the sensor-less case where saturation effect is automatically being considered in flux linkage calculations. The phase 1 torque in sensor case has been plotted for the three different dwell angles in Fig. 11 for making the comparison easy.

The results shown in Fig. 9 were taken for a load torque of 2 Nm. Considering the inductance profile of the machine, the current required for producing this torque could be calculated from Eqn (1) which comes close to 3 amp. The instantaneous current equation of the phase winding of the SRM can be written as

$$i = (V/R)(1 - e^{-t/\tau}) \quad (6)$$

where  $\tau$  is the time constant of the phase winding (where  $R=1 \Omega$  and  $L=10 \text{ mH}$ ). The time taken by the phase winding to reach the required exciting current for a supply voltage of 300 V can be calculated from the above equation. Considering the reference speed, this time can be translated into an appropriate  $\theta_{ON}$ . Similarly, an appropriate  $\theta_{OFF}$  can be arrived at by considering the maximum value of inductance and the phase current magnitude.

These work out to be about  $10^\circ$  and  $25^\circ$  respectively for 2 Nm and 50 rad/s. From the simulations, it is also found that minimum torque pulsations have been obtained for these values of  $\theta_{ON}$  and  $\theta_{OFF}$ . Adopting the above procedure,  $\theta_{ON}$  and  $\theta_{OFF}$  have been calculated for a load torque of 20 Nm with the rated torque of the motor being 25 Nm. The reference speed has been taken as 50 rad/s. The appropriate values were obtained as  $\theta_{ON}=8.9^\circ$  and  $\theta_{OFF}=22^\circ$  respectively. When the simulation was made with these values, the response was much better in terms of torque pulsations and speed profile (Figs 12(a) and (b) as compared to

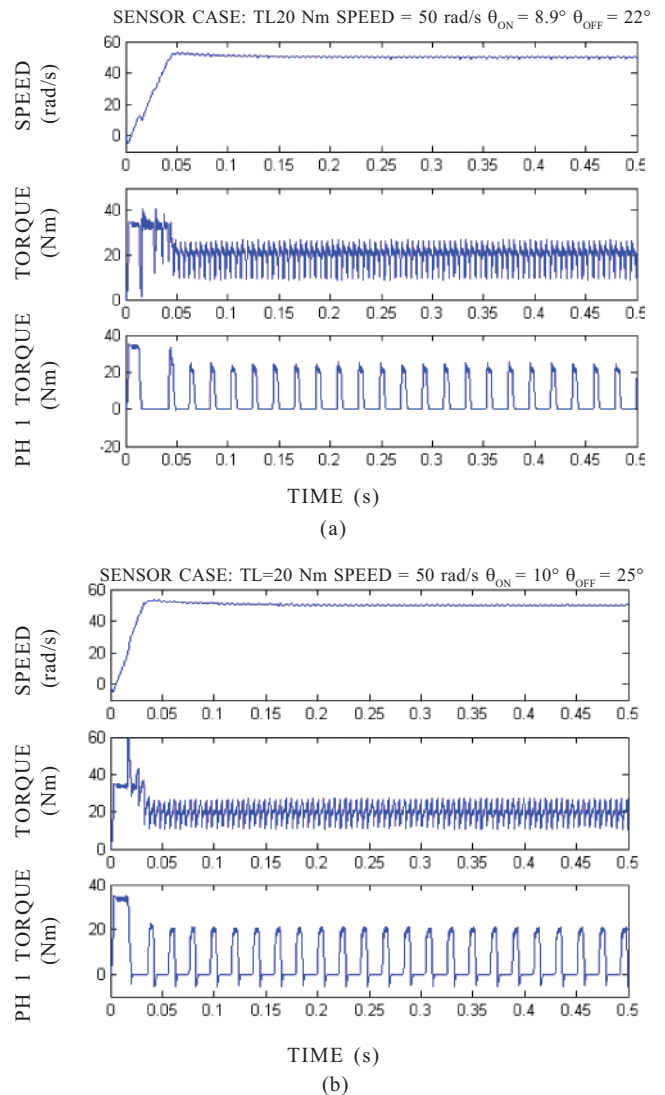


**Figure 12.** Responses of the SRM drive in sensor mode for a speed of 50 rad/s at a load torque of 20 Nm with different dwell angles (a and b).

different values of  $\theta_{ON}$  and  $\theta_{OFF}$  (that is  $\theta_{ON} = 10^\circ$  and  $\theta_{OFF} = 26^\circ$ ).

## 5. DISCUSSIONS

The foregoing analysis presents the results in both sensor and sensor-less modes of operation of SRM for different values of dwell angles and electromagnetic torques, especially for current chopping mode of SRM. In single-pulse mode, one can hardly have a control over the complete dwell angle as the rotation takes place at a very fast rate and the device turn-on ( $\theta_{ON}$ ) and turn-off ( $\theta_{OFF}$ ) have to be done within a very short span of time. It is clearly seen that the pulsations in torque are significantly affected by the period of conduction of the particular phase winding of the SRM drive in conjunction with its inductance profile. It is essential to bring the phase winding current to the maximum required value for a given load torque before the rotor poles start to align with the stator poles. So,  $\theta_{ON}$  has to be a little ahead of the point at which the inductance starts to rise. How ahead this point should be is decided by two factors: (a) the speed of the motor, and (b) the required current value for producing the demanded load torque value.

Similarly, the conducting phase has to be commutated before the inductance goes into decreasing mode. That is,  $\theta_{OFF}$  has to be ahead of the point from where the inductance starts to decrease. How ahead this point should be is decided again by the speed of the motor, the maximum value of inductance and the value of current through the phase winding. So, appropriate values of  $\theta_{ON}$  and  $\theta_{OFF}$  can be calculated if the present conditions of the motor are known so that torque pulsations can be minimised.

## 6. CONCLUSIONS

This paper presents the impact of dwell angle on the pulsations of the electromagnetic torque in a SRM drive. Detailed models have been implemented in Simulink/Matlab environment for both 'sensor and sensor-less' mode of operation of the SRM drive. The sensor-less mode of operation has been achieved by computing the flux linkages of the machine at various values of excitation currents and rotor positions from the finite element analysis

of the SRM using the FE package, Maxwell. The analysis is carried out for various values of dwell angle and for specific values of electromagnetic torque and speed. From these simulations, appropriate values of ON and OFF angles have been deduced. These values have been theoretically verified using the torque and current expressions for the SRM drive. To cross check the calculation procedure adopted for the dwell angle for a different value of torque, the dwell angle has been calculated using the same procedure and the analysis in Simulink environment has been done for this calculated condition. It is found that the torque pulsations are minimum with the calculated values of  $\theta_{ON}$  and  $\theta_{OFF}$  as compared to a different dwell angle. In all, the importance of dwell angle in the control of SRM has been brought out in this paper and a methodology has been advocated to calculate appropriate value of dwell angle for minimising torque pulsations.

## REFERENCES

1. Jain, Amit K. & Mohan, N. SRM power converter for operation with high demagnetisation voltage. *In IAS Annual Meeting*, 2004. pp. 1625-631.
2. Miller, T.J.E. (Ed). *Electronic control of switched reluctance machines*. Newnes Power Engineering Series, UK, 2001. ISBN 0 7506 50737.
3. Krishnan, R. *Switched reluctance motor drives: Modelling, simulation, analysis, design, and applications*. Industrial Electronics Series, CRC Press, 2001.
4. Ehsani, M., *et al.* Elimination of position sensors in switched reluctance motor drives: State of the art and future trends. *IEEE Tran. Indust. Elect.*, 2002, **49**(1), 40-47.
5. Fedigan, Stephen J. & Cole, Charles P. A variable-speed sensor-less drive system for switched reluctance motors. Texas Instruments Application Report SPRA600, October 1999.
6. Murphy, J.M.D. & Turnbull, F.G. *Power electronic control of ac motors*. Pergamon Press, 1989.
7. SIMULINK/MATLAB (ver 6.5) manual. Math works Inc, USA.

## Contributors



**Ms G. Bhuvaneshwari** obtained her Masters and Doctoral degrees from the Indian Institute of Technology (IIT) Madras, Chennai. She has been with the Department of Electrical Engineering, IIT Delhi, New Delhi, since 1997 as a faculty member. She is a senior member of IEEE, USA. Her areas of interest are power electronics, machines, drives, and power quality.

**Mr P. Srinivasa Rao** obtained his ME in Electrical Engineering, IIT Delhi, New Delhi, in 2003. He is currently working with Patni Computers in the area of embedded system design.

**Mr Sarit Guha Thakurta** obtained his BTech from IIT Delhi, New Delhi, and MS from ETH, Zurich, Switzerland. He is currently pursuing his studies at Indian Institute of Management, Kozhikode.



**Prof S.S. Murthy** is presently professor in the Department of Electrical Engineering, IIT Delhi, New Delhi. He is a fellow of IEE, UK, and a senior member of IEEE. He also served as the Director of NIT, Surathkal, for a period of two years. His areas of interest are induction generators, power electronics, and electric drives.